EXPERT OPINION

Investigation of a novel 3-fluid nozzle spray drying technology for the engineering of multifunctional layered microparticles

Ritesh M Pabari, Tara Sunderland & Zebunnissa Ramtoola†
†*School of Pharmacy, Royal College of Surgeons in Ireland, Dublin 2, Ireland*

Objective: To examine the potential of a novel 3-fluid nozzle spray drying technology to formulate differentiated layered microparticles (MPs) of diclofenac sodium (DFS)/ethyl cellulose (EC).
Methods: DFS/EC MPs were formulated using the inner and/or outer nozzles of a novel 3-fluid nozzle and compared with MPs formed using conventional (2-fluid) spray drying. MPs were characterised for particle size and for morphology by TEM and SEM. Distribution of DFS and EC of MPs was analysed by FT-IR and DSC. A two-factor, three-level (3^2) factorial design was applied to investigate the effect and interaction of total feed solid content (TSC) and feed flow rate (FFR) on MP size, $D_{50\%}$ and $D_{90\%}$, bulk density and MP yield.
Results: Interestingly, TEM demonstrated that MPs formed by 3-fluid nozzle spray drying showed a heterogeneous internal morphology consisting of a core and coat, characteristic of a microcapsule. In comparison, MPs from conventional spray drying showed a homogeneous internal morphology, characteristics of a matrix system. This differential distribution of DFS/EC was supported by FT-IR and DSC. Results of multiple linear regression analysis showed a linear relationship for the effect of TSC and FFR on all responses except for $D_{50\%}$ where a quadratic model was valid. The effect of TSC/FFR on MP size and yield was similar to conventional spray drying.
Conclusion: The novel 3-fluid nozzle spray drying offers a new method of designing layered microparticles or microcapsules which can have wide applications from drug stabilisation to controlled drug delivery and targeting.

Keywords: 2-fluid nozzle, 3-fluid nozzle, diclofenac sodium, ethyl cellulose, factorial design, spray drying

Expert Opin. Drug Deliv. (2012) 9(12):1463-1474

1. Introduction

Microencapsulation is a technique widely used in the pharmaceutical industry for a number of applications including controlled drug release, targeted drug delivery and taste masking [1]. Numerous microencapsulation techniques have been developed over the years and these range from solvent evaporation from emulsions to coacervation-phase separation, coating of non-pareil beads and spray drying. Microencapsulation of pharmaceutical actives using spray drying is a well-established method and the formulation and process parameters influencing microencapsulation have been studied extensively [2-4]. The spray drying process generally consists of atomising the feed fluid through a nozzle to form fine droplets which are dried in a stream of hot drying air or nitrogen. The dried particles are separated from the drying medium and are collected into a collecting vessel [5,6].

The atomiser/nozzle plays a very important role in defining the droplet size formed hence the particle size and size distribution of the product and various types of nozzles, ranging from single fluid to 4-fluid nozzles, centrifugal wheel rotary atomizer, rotating disc atomizer and ultrasonic nozzle have been investigated [7-12].

Of these, the 2-fluid (2-F) nozzle is the most commonly used for the formulation of microparticles for various applications. Considerable data have been published to date on the effect of process and formulation variables on the characteristics of the resultant microparticles [4,13-15]. A change in the feed flow rate was reported to directly influence the particle size, and inversely influence the particle size distribution, particle morphology and product recovery [13]. Similarly, an increase in the total solid content of feed solutions was reported to directly impact microparticle size. Clarke *et al.* reports that for the biodegradable PLA and PLGA polymers, polymer molecular weight and concentration were important factors influencing microparticle formation and observed an increase in microparticle size with increasing polymer concentration [15].

In general, spray-dried microparticles (MPs) or microspheres of drug and polymer tend to consist of a matrix structure where the drug is distributed within the polymer matrix and serve the purpose of protection/stabilisation or controlled release of the actives [4,13]. As the active in a microparticle matrix structure is usually distributed throughout the particle, it is present at the particle surface and gives rise to a fast initial or burst drug release. Similarly, such surface exposure of drug potentially leads to degradation of labile molecules [14,16]. For efficient sustained release of drug from MPs, microcapsule formation is reported to be desirable [17]. Similarly, microcapsules would be desirable for protection of labile molecules. The co-axial nozzle systems have been previously reported for microcapsule production by the method of electrospraying giving high yield and particles of uniform size distribution [18].

A novel 3-fluid nozzle has been reported earlier by Legako *et al.* [19]. for the formulation of microcapsules of whey protein solution and fish oil. Application of the 3-fluid nozzle to the formulation of drug polymer microparticles is novel and was first described by Ramtoola *et al.* [20].

In this study, we examined the potential of a novel 3-fluid (3-F) nozzle spray drying to form two-layered MPs or microcapsules. It is envisaged that as a result of the nozzle configuration, which allows the feeding of two separate concentric streams of the active and polymer solutions [20], the drug and polymer solutions will form a two-layered droplet at the nozzle tip to give MPs with internal morphology similar to a microcapsule (**Figure 1A**). In comparison, using the 2-F nozzle, the drug/polymer solution generally formulated as one feed solution is fed through a single feed line and sprayed through a single nozzle (**Figure 1B**) to result in a matrix type of particles.

The characteristics and internal morphology of MPs formulated using the novel 3-F nozzle was first examined and compared with MPs formed using 2-F nozzle spray drying. Diclofenac sodium (DFS), a non-steroidal anti-inflammatory analgesic drug was used as a model drug and ethyl cellulose, an inert hydrophobic polymer, was used as the encapsulating polymer. A two-factor, three-level (3^2) factorial design and response surface methodology were applied to derive statistical models to investigate the relative significance of two variables, total solid content of the feed solution (X1) and feed flow rate (X2) and their interaction on the responses, i.e., median microparticle size, $D_{50\%}$ (Y1), microparticle size at which 90% of the particles are below, $D_{90\%}$ (Y2), bulk density (Y3) and microparticle yield (Y4).

2. Materials and methods

2.1 Materials

Diclofenac sodium (DFS) USP grade was bought from Dipharma Francis, Italy. Ethyl cellulose (EC) (45cP) was bought from Sigma-Aldrich, Ireland. Ethanol (EtOH) Reagent grade was bought from Lennox, Ireland.

2.2 Preparation of the spray-dried microparticles

Feed solutions containing diclofenac sodium (DFS) or ethyl cellulose (EC) as two individual solutions were spray-dried (Buchi Mini Spray dryer, Model B-290 (Buchi Switzerland)) using a novel 3-F nozzle. The DFS solution was fed through the inner core of the nozzle using a second pump (Ecoline pump, Ismatec), whereas the EC solution was fed through the second or outer feed layer of the 3-F nozzle. Fluidising nitrogen was fed through the third nozzle. The feed flow rate (FFR) of DFS and ethanolic solutions were maintained at the same rate and were in the range 2 – 8 mL/min. The total solid content (TSC) of each feed solutions used were 2.5, 5 or 10% w/v. The inlet temperature (Tinlet) was set at 80°C and the air (in this case nitrogen) aspiration rate was controlled at 100%. This nitrogen drying gas carries the spray-dried microparticles to the cyclone separator and subsequently to the collector from where the microparticles are recovered. Flow rate of fluidising nitrogen was maintained at 400 Nl/h. Outlet temperatures were monitored during the spray-drying process. The dry product was collected and weighed and product yield (%) was calculated as (weight of the spray – dried product/total solids in the feed solution) × 100.

MPs were also prepared by spray drying using the standard 2-F nozzle. Feed solutions in this case consisted of a single solution of DFS and EC in ethanol at 2.5, 5 or 10% w/v TSC using a feed flow rate of 2 – 8 mL/min. The process parameters used were as described for the 3-F nozzle.

2.3 Characterisation of spray-dried microparticles

2.3.1 Microparticle size analysis and bulk density

The particle size and size distribution of the spray-dried MPs was measured using the Mastersizer 2000 (Malvern Instruments, Malvern, Worcestershire, UK). The microparticles were measured for size in the dry state using the dry dispersion attachment (Scirocco™). Briefly, a small amount of

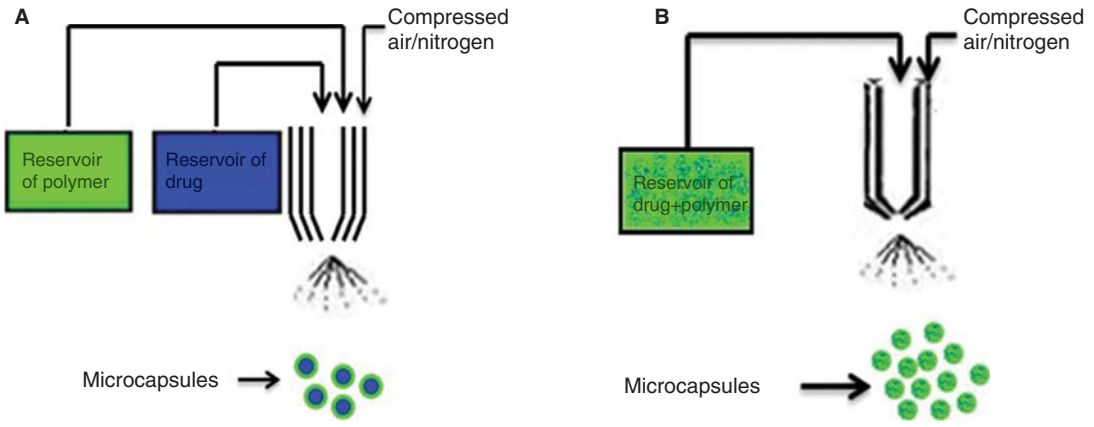

Figure 1. Diagrammatic representation of spraying and droplet/MP formation from (A) a novel 3-F nozzle and (B) conventional 2-F nozzle.

sample was placed onto the sample tray of the dry powder cell and measured for $D_{10\%}$, $D_{50\%}$, $D_{90\%}$.

The bulk density (g/cc) was calculated from the accurately weighed MPs (g) and the corresponding bulk volume (cc) measured using a graduated cylinder.

2.3.2 *Morphology*

External morphology of the MPs was evaluated by a variable pressure field emission scanning electron microscope (SEM) (Hitachi Scanning Electron Microscope (model S 3500N, Japan). Samples were mounted on double-sided adhesive tape attached to an aluminium stub and were sputter-coated with gold to approximately 30 nm (Polaron SC500, Gold Sputter Coater, Quotum Technologies, Newhaven, UK) [21]. Internal morphology of MPs was investigated by transmission electron microscope (TEM) (Hitachi- 7650 with a side mount 2k AMT camera). Dry microparticle samples were mounted onto Pioloform mesh copper grids with or without 2% phosphotungstic acid (PTA) for negative staining. The grids were observed under the TEM operated at 100 kV. Images were taken at 7 k or 10 k magnifications.

2.3.3 *Drug loading and encapsulation efficiency*

Accurately weighed MPs (~ 5 mg) were dissolved in 2 ml ethanol by sonication for 30 min and phosphate-buffered saline at pH 6.8 was then added to precipitate the EC polymer. After centrifugation, 1 ml aliquot of the supernatant was diluted with 10 ml of pH 6.8 and the absorbance was then measured using UV Spectroscopy (Libra S22, Biochrom, UK) at λ_{max} 276 nm. The drug content of the samples was then calculated using a standard calibration curve for DFS in the concentration range of 0.005 – 0.05 mg/ml. The drug assay method was verified using physical mixtures of DFS and EC and showed 100% drug extraction. In addition, the UV scan for EC solutions showed no absorbance over the 250 – 400 nm range and hence no interference with the DFS absorbance at 276 nm.

The percent drug loading of the MPs and encapsulation efficiency (EE) of DFS in the MPs were calculated by:

$$\%\ \text{DFS loading} = (\text{amount of DFS in MPs/weight of MPs}) \times 100.$$

$$\%\ \text{EE} = \left(\begin{array}{l}\text{assayed drug content per 5 mg of MPs /}\\ \text{theoretical drug content per 5 mg of MPs}\end{array}\right) \times 100.$$

2.3.4 *Fourier transform infra-red spectroscopy*

Fourier Transform Infra-Red (FT-IR) spectroscopy spectra were obtained using a Bruker Tensor 27 FT-IR spectrometer (Bruker Optics, Ettlingen, Germany) equipped with DTGS detector. The background scan was performed prior to analysis. The spectra were an average of 32 scans at a resolution of 4 cm^{-1} over the frequency range of 4000 – 400 cm^{-1}. KBr discs were prepared using a manually operated hydraulic press (Specac, Kent, UK). Analysis of the spectra was performed using the OPUS Data Collection Program (V 1.1). The samples for infra-red analysis and the KBr were dried for at least an hour prior to analysis in a drying oven (Specacabinet, Kent, UK) at 32 ± 0.5°C.

2.3.5 *Differential scanning calorimetry*

Differential scanning calorimetry (DSC) analysis was carried out on spray-dried MPs using a DSC Q100 V9.0 Build 275, with a recirculation cooling system (TA Instruments, New Castle, Delaware, USA). Samples were accurately weighed and sealed in aluminium pans. An empty aluminium pan was used as the reference. The analysis was performed under a purge of dry nitrogen. Samples were heated by a ramp method at a rate of 10°C/min over the temperature range 10 – 300°C and the thermograms examined for phase changes/evidence of degradation. DSC was also carried out on the unprocessed DFS, EC and 1:1 physical mixture (PM) of the DFS and EC. The temperatures at which thermal events were observed were recorded. Calibration of the instrument was performed with indium reference standard prior to the start of the study.

Table 1. Variables in 3^2 full factorial design.

Independent variable, factor	Levels used		
	Low (-1)	Middle (0)	High (1)
X1; Total solid content (%)	2.5	5	10
X2; Feed flow rate (mL/min)	2:2	4:4	8:8
Dependent variable, response			
Y1 = microparticle size ($D_{50\%}$) (μm)			
Y2 = microparticle size ($D_{90\%}$) (μm)			
Y3 = bulk density (g/cc)			
Y4 = microparticle yield (%)			

Table 2. Matrix of 3^2 full factorial design.

Exp. No	Total solid content (X_1)	Feed flow rate (X_2)
1	-1	0
2	0	0
3	0	1
4	-1	1
5	1	1
6	1	-1
7	0	-1
8	1	0
9	-1	-1

2.3.6 *Experimental design*

Factorial design and response surface methodology was used to determine the significance of each independent factor studied and their interaction over the considered responses. It can be used to find the best combination of a given set of factors, which give an optimal response [22]. In this study, it was applied to evaluate the effect of the independent formulation and process factors of total solid content (X1) and feed flow rate (X2) and their levels and interaction on the resultant microparticle size, density and particle yield (Y1 – Y4) and hence allow selection of optimum parameters for desirable MP properties. The independent variables studied, their levels and responses measured are shown in **Table 1**.

The matrix of the factorial design is outlined in **Table 2**. Each row in the matrix represents an experiment and each experiment presents a set of results, i.e., four responses or dependent variables studied. The selected levels are within the practical use and were chosen to have a measurable effect on the response.

3. Results

3.1 Evaluation of novel 3-fluid spray drying nozzle for microcapsule engineering

Droplet and particle formation using the 3-F nozzle was first investigated. MPs formed by feeding DFS or EC solution, at 5% w/v, through inner or outer layer of the 3-F nozzle, respectively, at increasing feed flow rate (FFR) were compared with corresponding MPs formed using the 2-F nozzle (**Table 3**). MPs were subsequently formulated using both inner and outer nozzles of the 3-F nozzle simultaneously (**Table 3**). Spray-dried MPs were formed in all cases. Particle yield decreased with increasing FFR. A lower yield of 32 – 47% was obtained for the 3-F nozzle compared to 2-F nozzle (66 – 74%). Highest yield was obtained at the lowest FFR of 2 mL/min for both nozzles (47% and 74%), while at higher FFR, particularly at 8 mL/min, yield was reduced (35% – 66%).

Increasing the FFR from 2 to 8 mL/min did not affect median particle size of particles prepared using the 2-F nozzle or the inner core of the 3-F nozzle (**Table 3**). An increase in the $D_{90\%}$ value (from 18 – 26 μm to 33 – 65 μm) was however observed at the highest FFR of 8 mL/min for both nozzle types. Particle size of MPs prepared using the outer layer of the 3-F nozzle was observed to decrease ($D_{10\%}$, from 6.2 to 3.4 μm; $D_{50\%}$, from 14.2 to 6.9 μm; $D_{90\%}$ from 31 to 15 μm) with increasing FFR (from 2 to 8 mL).

MPs from the 3-F nozzle showed a defined core and coat internal morphology, similar to a microcapsule (**Figure 2A**). This is contrast to DFS and EC MPs from the standard 2-F nozzle, which showed a homogeneous internal morphology, representative of a matrix system (**Figure 2B**). MPs from outer 3-F nozzle appeared hollow and collapsed (**Figure 2C**).

3.1.1 *Fourier Transform Infra-Red (FT-IR) spectroscopy*

FT-IR analysis of DFS shows characteristics peaks at 3388 cm^{-1} and 3258 cm^{-1} corresponding to NH stretching of its secondary amine and amide band II, respectively, strong -C = O peak at 1791 cm^{-1} and -C-O peak at 1247 cm^{-1}. The shoulder peak at 1669 cm^{-1} and peak at 892 cm^{-1} can be related to the aromatic ring whereas the peak at 1168 cm^{-1} was attributed to aromatic C-Cl (**Figure 3A**). These were consistent with the literature [23-25]. These DFS peaks were observed in the 1:1 PM of DFS with EC (**Figure 3B**). The peaks relating to aromatic ring and aromatic C-Cl of DFS were clearly visible in MPs prepared using 2-F nozzle, interestingly, these peaks were either absent or subdued in MPs prepared using 3-F nozzle.

FT-IR for EC was reported to show a small but not sharp peak at 2950 cm^{-1} attributed to asymmetric structure vibrations of the -OC2H5 ethoxy groups [26], and broad distinct peak near 1100 cm^{-1} corresponding to the C-O-C stretch in the cyclic ether [27,28]. Both these events are observed in the FTIR of

Table 3. Characteristics of DFS/EC spray-dried microparticles using a 2-fluid (2-F) or 3-fluid (3-F) nozzle at a feed concentration of 5%w/v.

Nozzle used	FFR (mL/min)	T_{Outlet} (°C)	$D_{10\%}$ (μm)	$D_{50\%}$ (μm)	$D_{90\%}$ (μm)	Yield (%)
Inner 3-F	2	43	5.8 ± 0.1	14.6 ± 0.4	33.0 ± 2.9	47.2
Inner 3-F	4	52	5.6 ± 0.2	13.5 ± 0.7	30.4 ± 3.0	35.9
Inner 3-F	8	50	5.0 ± 0.0	13.0 ± 0.1	65.7 ± 7.9	35.0
Outer 3-F	2	53	6.2 ± 0.2	14.2 ± 0.2	31.4 ± 1.8	47.4
Outer 3-F	4	50	3.8 ± 0.1	8.3 ± 0.0	19.7 ± 1.5	32.0
Outer 3-F	8	39	3.4 ± 0.0	6.9 ± 0.0	15.0 ± 0.6	36.8
2-F	2	55	2.4 ± 0.0	7.0 ± 0.1	18.8 ± 1.6	74.4
2-F	4	53	2.1 ± 0.0	5.3 ± 0.1	11.6 ± 0.2	73.6
2-F	8	35	4.6 ± 0.1	9.9 ± 0.2	26.5 ± 3.4	66.2
3-F	4:8	46	2.5 ± 0.1	8.9 ± 0.2	24.8 ± 0.6	42.7
3-F	8:4	41	2.5 ± 0.1	7.4 ± 0.1	19.7 ± 1.0	40.2

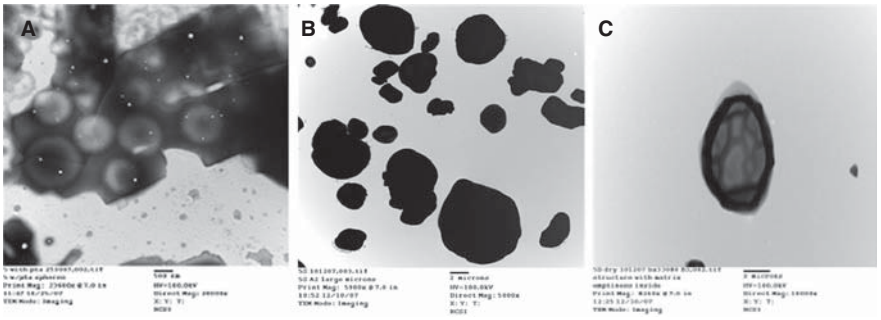

Figure 2. Internal morphology of MPs prepared by spray drying (A) EC solution through the outer and DFS solution through the inner core of the 3-F nozzle, (B) DFS and EC solution through the 2-F nozzle and (C) EC solution through the outer core of the 3-F nozzle.

MPs prepared using either 2-F or 3-F nozzle, however these peaks were stronger in intensity in the FTIR of MPs from 3-F.

To investigate the mechanism of particle formation, droplet formed through the 3-F nozzle was visualized at a low flow rate of ~ 0.5 mL/min, using a rhodamine solution as core solution through the inner nozzle, and a clear polymer solution through the outer nozzle. The droplet formed at the tip of the nozzle showed a pink-coloured core droplet within a clear outer polymer coat (**Figure 4A**); in contrast, the droplet formed at the tip of the 2-F nozzle using a rhodamine and polymer solution was homogeneous and darker in colour (**Figure 4B**).

3.2 Effect of formulation and process variables on microcapsule characteristics and morphology

3.2.1 Statistical analysis and mathematical modelling

The influence of increasing total solid content (X1) of the feed solution and feed flow rate (X2) on the microparticle characteristics was analysed by response surface modelling using the Design-Expert® software. The values for the responses, Y1 = median microparticle size ($D_{50\%}$), Y2 = the size at which 90% of MPs are below ($D_{90\%}$), Y3 = bulk density, Y4 = microparticle yield are shown in **Table 4**. The statistical models were developed based on the regression analysis of statistically significant variables and the results for each response variable derived by the best fit method are shown in equations (1) – (4) below.

$$Y1(D_{50\%}) = +7.47639 + 0.66186 * X1 - 1.30925 * X2 - 0.082310 * X1 * X2 - 0.015378 * X1^2 + 0.22704 * X2^2 \quad (1)$$

$$Y2(D_{90\%}) = -0.16333 + 2.17657 * X1 + 2.65714 * X2 \quad (2)$$

$$Y3(\text{bulk density}) = +0.15736 + 6.09905E-003 * X1 - 4.12771E-003 * X2 \quad (3)$$

$$Y4(\text{microparticle yield}) = +88.74222 - 2.51924 * X1 - 5.57316 * X2 \quad (4)$$

Equations (1) – (4) demonstrate the quantitative effect of the formulation and process variables; total solid content (X1) and feed flow rate (X2) and their interactions on the responses Y1 – Y4. Analysis of variance (ANOVA) for the responses showed that the quadratic regression model was significant and valid for the effect of TSC or FFR on response Y1 ($p = 0.0106$), while linear regression model was valid for the

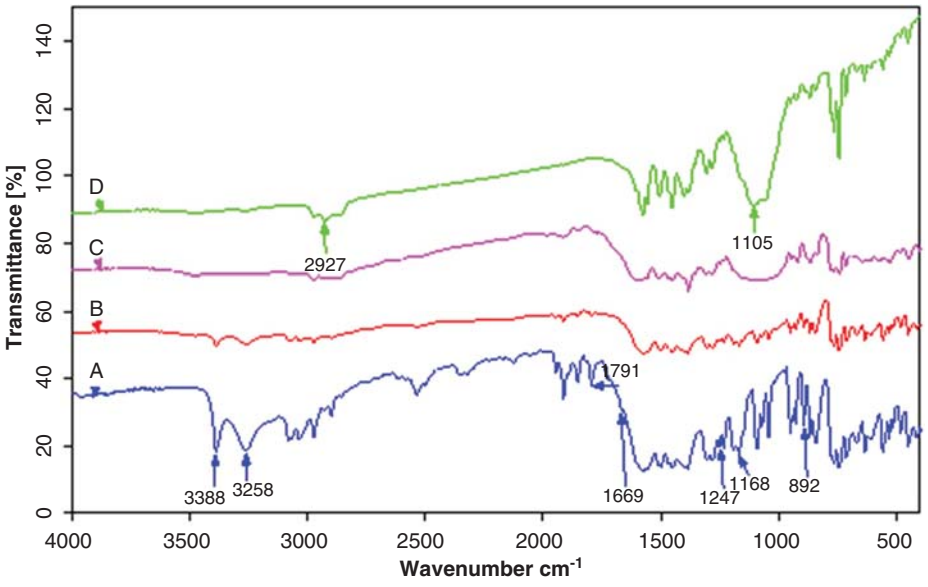

Figure 3. FTIR spectrum of (A) diclofenac sodium (DFS), (B) physical mixture of diclofenac sodium and ethyl cellulose, (C) MP prepared using a 2-F nozzle, (D) MP prepared using a 3-F nozzle.

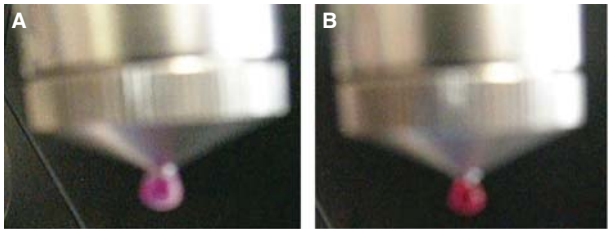

Figure 4. Morphology of rhodamine and EC polymer droplets formed through the (A) 3-F nozzle and (B) 2-F nozzle.

effect of TSC or FFR on each of the responses Y2 ($p = 0.0003$), Y3 ($p < 0.0083$) and Y4 ($p = 0.0063$) ($p < 0.05$) and hence was suitable to represent the observed MP characteristics and serve as a response predictor. The statistical analysis for the response surface quadratic/linear model showed that the standard error of estimate for Y1 was 0.56, Y2 was 1.12, Y3 was 4.637E-003 and Y4 was 3.40 demonstrating good fit of the model.

A positive regression coefficient of variable X1 in equations (1) – (3) indicates that an increase in TSC resulted in an increase in MP size and bulk density. The regression coefficient of variable X2 was negative in equations (1) and (3) and positive in equation (2) indicating a decrease in $D_{50\%}$ and bulk density, but an increase in $D_{90\%}$, with an increase in FFR. The negative regression coefficient for X1 and X2 in equation (4) indicates a decrease in MP yield with an increase in TSC or FFR.

In equation (1), the higher-order factors ($X1^2$ and $X2^2$) and coefficients with both factors (i.e., X1X2) denote a quadratic relationship and an interaction effect of both factors on median particle size. A positive regression coefficient for the quadratic term $X2^2$ indicates that median MP size decreased with decreasing FFR, to a minimum after which median MP size increased.

3.2.2 *Analysis of the fitted data – microparticle size; $D_{50\%}$ (Y1), $D_{90\%}$ (Y2), bulk density (Y3) and yield (Y4)*

The relationship between the dependent variables; MP size, $D_{50\%}$ (Y1), and $D_{90\%}$ (Y2), bulk density (Y3) and MP yield (Y4) and the independent variables; total solid content (TSC) (X1) and feed flow rate (FFR) (X2) is demonstrated on the response surface plots in **Figure 5A – D**. The plots also show the region of maxima (region in red) and minima (region in blue) for each of the four responses investigated. Quality of fit of the model for each response showed an R^2 value of 0.9784, 0.9318, 0.7973 and 0.8156 for Y1, Y2, Y3 and Y4, respectively.

An increase in FFR to 8 mL/min led to ~ 2-fold increase in the particle size ($D_{50\%}$ and $D_{90\%}$) and a decrease in yield and density, regardless of the TSC (**Figure 5A – D**). **Figure 5A** also illustrates a quadratic relationship for the effect of FFR on median MP size. An increase in FFR resulted in a small decrease in the median MP size from 7 – 9 µm to 6 – 7 µm after which median MP size increased to 11 – 13 µm. Both the TSC and FFR effect were contributory resulting in highest $D_{90\%}$ and lowest MP yield at the highest FFR and TSC.

A linear relationship for the effect of FFR and TSC was observed on bulk density (Y3) and product yield (Y4) (**Figure 5C, D**). An increase in FFR resulted in a decrease in bulk density while an increase in TSC resulted in an increase in bulk density. Increase in FFR and TSC resulted in a decrease in yield, with minimum yield at highest TSC and FFR.

Table 4. Microparticle characteristics prepared by using a 3-F nozzle and 2-F nozzle.

Exp no.	X1 (%)	X2‡ (mL/min)	To (°C)	$D_{50\%}$ (μm)	$D_{90\%}$ (μm)	SPAN	Yield (%)	Density (g/cc)
9	2.5	2:2	52	7.04 ± 0.19	15.60 ± 0.40	1.84 ± 0.03	67.6	0.164
1	2.5	4:4	45	6.94 ± 0.08	16.12 ± 0.88	1.95± 0.11	65.0	0.162
4	2.5	8:8	42	12.87 ± 0.48	29.74 ± 1.80	1.88 ± 0.01	16.6	0.114
7	5	2:2	51	7.07 ± 0.23	16.14 ± 0.07	1.91 ± 0.08	69.2	0.183
2	5	4:4	45	7.39 ± 0.12	17.52 ± 1.13	1.99 ± 0.18	57.8	0.166
3	5	8:8	43	13.32 ± 0.87	32.36 ± 2.83	5.32 ± 3.29	33.9	0.173
6	10	2:2	53	9.37 ± 0.24	25.24 ± 1.62	1.79 ± 0.13	40.7	0.201
8	10	4:4	45	7.23 ± 0.48	36.27 ± 14.2	4.62 ± 1.59	37.5	0.201
5	10	8:8	45	11.31 ± 0.17	46.57 ± 3.04	4.64 ± 0.19	20.5	0.182
-	2.5	8*	54	6.75 ± 0.23	15.75 ± 0.39	2.04 ± 0.03	91.2	0.223
-	5	8*	35	9.86 ± 0.23	26.52 ± 3.37	2.22 ± 0.29	66.2	0.175
-	10	8*	48	12.52 ± 0.54	40.48 ± 4.98	2.87 ± 0.27	29.0	0.173

*FFR through 2-F nozzle.

‡FFR through the inner nozzle:FFR through the outer nozzle of the 3-F nozzle.

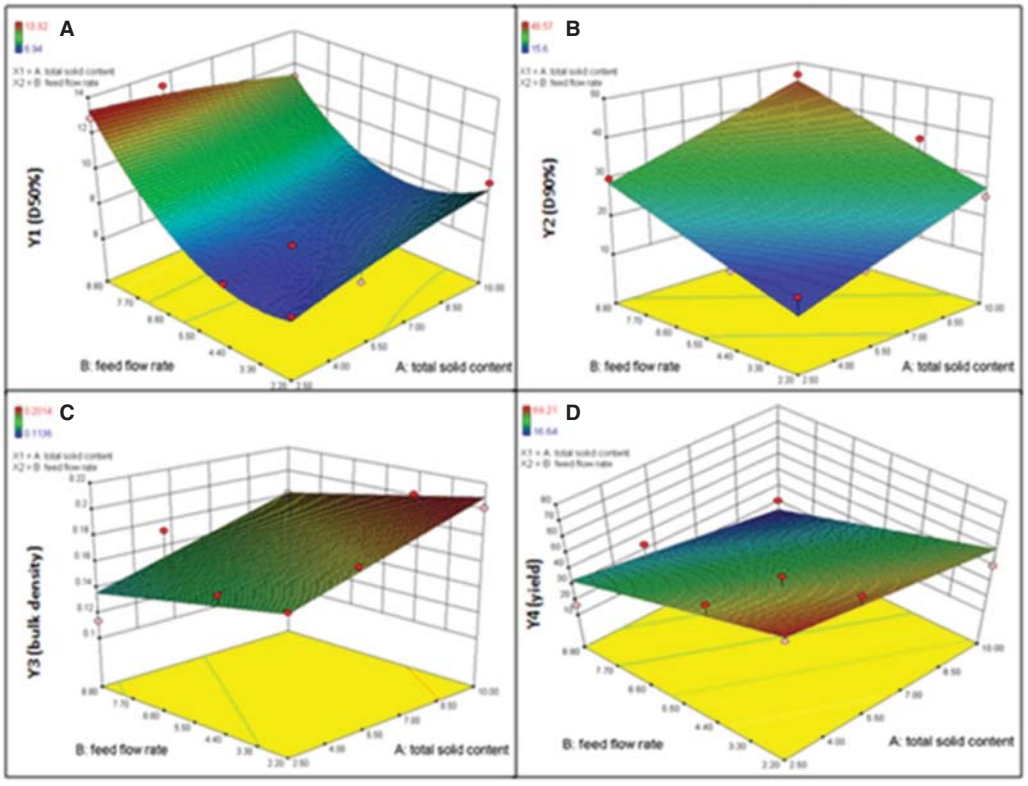

Figure 5. Response surface plot showing the effect of X1 (total solid content) and X2 (feed flow rate) on microparticle characteristics (A) Y1 (median size, $D_{50\%}$), (B) Y2 (size, $D_{90\%}$), (C) Y3 (bulk density), (D) Y4 (microparticle yield). (*feed flow rate (FFR) A:A is represented as A.A).

3.3 Comparison of microparticle characteristics: 3-fluid nozzle vs 2-fluid nozzle

The characteristics of MPs generated using the 3-F nozzle were compared with those of MPs formulated using a conventional 2-F nozzle at a FFR of 8 mL/min (**Table 4**). MP size was similar for both nozzle types. An increase in TSC resulted in an increase in both, $D_{50\%}$ and $D_{90\%}$ of the MPs from the 2-F nozzle, while for 3-F MPs only $D_{90\%}$ increased with an increase in TSC. At lower TSC of 2.5%, MPs from 2-F nozzle was denser and showed higher product yield compared to the MPs from 3-F nozzle. An increase in TSC to 10% resulted in a decrease in bulk density and yield of 2-F MPs.

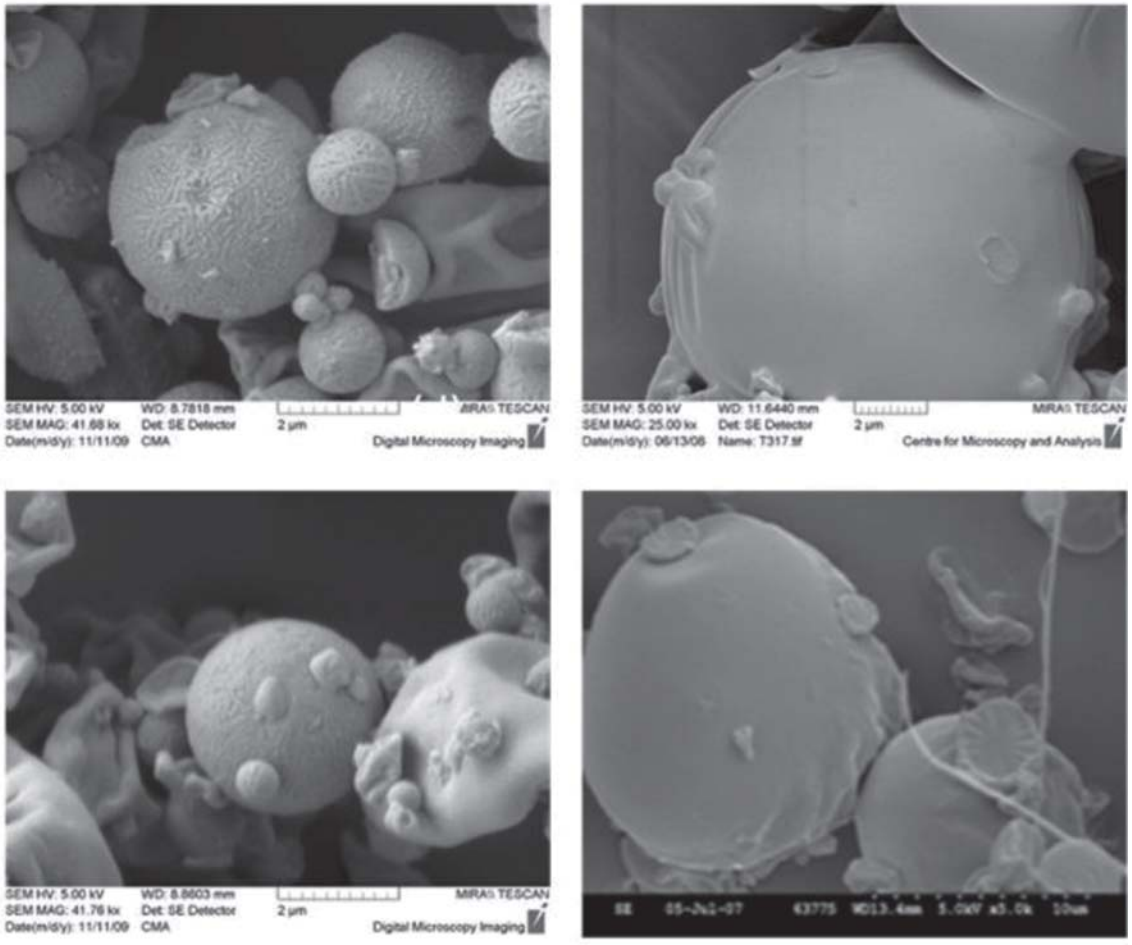

Figure 6. Electron micrographs of MPs prepared using the 3-F nozzle at TSC of 5% and FFR of (A) 2:2 mL/min, (B) 8:8 mL/min, at (C) TSC of 10% and FFR of 2:2 mL/min and (D) 2-F nozzle at TSC of 10% and FFR of 7 mL/min.

Consequently, at higher TSC of 10%, MPs from 3-F nozzle was denser and showed higher product yield compared to the MPs from 2-F nozzle.

MPs prepared using 3-F nozzle showed high encapsulation efficiency (EE) in the range of 101 – 119%, while EE of DFS in MPs using the 2-F nozzle was in the range 95.12 – 99.36%.

3.4 Morphology of microparticles

External morphology of MPs prepared using the 3-F nozzle was similar across the FFR and TSC examined and to the morphology of MPs from the 2-F nozzle (**Figure 6A – D**).

3.5 Differential scanning calorimetry (DSC)

DSC studies of unprocessed DFS and spray-dried DFS showed an endothermic peak at 293°C and 289°C, respectively, indicative of its melting point (**Figure 7A**), consistent with literature reports [29,30]. Unprocessed EC showed a broad endotherm from ~ 37 to ~ 112°C, probably due to increase in molecular mobility (**Figure 7B(b)**) [31,32]. Similarly, spray-dried EC showed a broad endotherm, however, followed by a small endothermic event at ~ 130°C, which could be due to the Tg of EC at around 135°C as reported by Rekhi *et al.* [33]. The events at ~ 175°C and ~ 218°C were related to oxidative degradation of EC at elevated temperatures [25,32]. PM of EC with DFS showed just a broad endotherm, similar to that observed for spray-dried EC. However, at a temperature of above 250°C, a degradation event was observed, probably related to the degradation of DFS [34].

Interestingly, the DSC thermogram of MPs spray-dried using 3-F nozzle was different to those of MPs prepared using 2-F nozzle. For 3-F nozzle MPs, the broad endothermic event observed at ~ 37 – 110°C was similar to that observed for spray-dried EC. This was followed by an endothermic peak for DFS at ~ 262°C, before degradation. The thermal profiles were consistent for 3-F nozzle MPs, regardless of the TSC or FFR (**Figure 7C and D**). MPs prepared by using 2-F nozzle showed a broader endothermic event, between ~ 37 and 150°C, compared to spray-dried EC. This broader event may represent increased solvent residuals or can be related to DFS distribution within the EC matrix which interferes

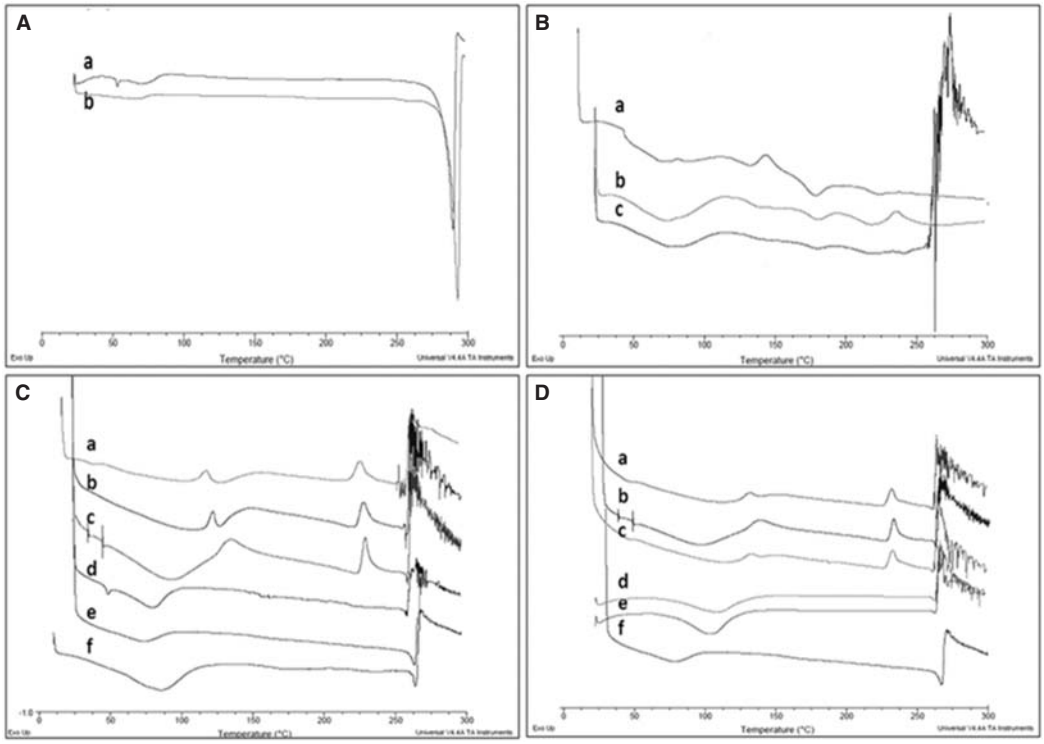

Figure 7. DSC thermograms of (A) (a) DFS and (b), spray-dried DFS (B) (a) spray dried EC, (b) unprocessed EC, and (c) 1:1 EC: DFS physical mix (C) MPs formulated at FFR of 8 mL/min from 2-F nozzle at TSC of (a) 2.5, (b) 5, and (c) 10% w/v and from 3-F nozzle at TSC of (d) 2.5%, (e) 5% and (f)10% w/v (D) MPs spray-dried at TSC of 5% w/v using the 2-F nozzle at FFR of (a) 2 (b) 4 (c) 8 mL/min, and the 3-F nozzle at FFR of (d) 2 (e) 4 and (f) 8 mL/min.

with EC mobility. This was followed by an exothermic event at ~ 225°C, possibly related to the re-crystallisation of DFS, before the degradation event observed at above 250°C.

3.6 Validation of the model

Theoretical (predicted) values of responses Y1 (particle size, $D_{50\%}$), Y2 (particle size, $D_{90\%}$), Y3 (bulk density), Y4 (microparticle yield) for the nine experiments were calculated from the response surface models; equations (1) – (4), respectively, by substituting values of X1 (total solid content) and X2 (feed flow rate). Good correlation between theoretical (predicted) values and the observed (actual) values was found for all the four responses of Y1 – Y4 (**Table 5a** and **b**). A batch containing 5% TSC was reformulated at the FFR of 8:8 mL/min. The particle size $D_{50\%}$ and $D_{90\%}$ of reformulated batch was found to be 7.13 ± 0.32 and 40.6 ± 24.78 µm, respectively, the bulk density was 0.1728 g/cc and product yield was 33.94%.

4. Discussion

Spray-dried MPs were formed irrespective of the type of nozzle used. MPs formed using the 2-F nozzle were smaller than corresponding MPs formed using the inner core of the 3-F nozzle. This was related to the different feed solutions used as the internal diameter of both nozzles was similar. A single DFS/EC solution was used for the 2-F nozzle while only DFS solution was used for the inner 3-F nozzle and this may have resulted in particle agglomeration of the DFS crystals formed on spray drying. MP size from 3-F nozzle was larger probably resulting in product settling in the spray-drying chamber, and hence less product being carried by the air aspiration to the cyclone separator and collecting vessel, resulting in lower product yield.

Increasing the FFR from 2 to 8 mL/min did not affect the size of MPs from the 2-F nozzle or inner core of the 3-F nozzle (**Table 3**), however a decrease in MP size with increasing feed flow rates was observed when using the outer layer of the 3-F nozzle. TEM showed these particles to be hollow (**Figure 2C**), hence they tend to collapse with increasing FFR resulting in a decrease in the MP size.

TEM studies showed that MPs prepared from 3-F nozzle had a defined core and coat, similar to a microcapsule, while using the standard 2-F nozzle a homogeneous internal morphology was observed. FT-IR analysis showed that MPs from 3-F nozzle were different to MPs from 2-F nozzle. FT-IR spectrum of 3-F nozzle MPs showed EC peaks that were stronger in intensity compared to the 2-F MPs. This was related to the fact that MPs prepared using 3-F nozzle has a coat of EC. MPs from the 2-F nozzle showed a similar FT-IR spectrum to 1:1 PM indicating a more homogeneous

Table 5a. Theoretical (predicted) values and the observed (actual) values observed for responses Y1 (microparticle size, $D_{50\%}$) and Y2 (microparticle size $D_{90\%}$)

	Y1 (Microparticle size $D_{50\%}$ (μm))			Y2 (Microparticle size $D_{90\%}$ (μm))		
	Actual value	Predicted value	Residual	Actual value	Predicted value	Residual
1	7.04	6.80	0.24	15.60	11.12	4.48
2	9.37	7.71	-0.64	16.14	16.57	-0.43
3	7.07	8.96	0.41	25.24	27.45	-2.21
4	6.94	6.76	0.18	16.12	16.97	-0.85
5	7.39	7.23	0.16	17.52	22.41	-4.89
6	7.23	7.57	-0.34	36.27	33.29	2.98
7	12.87	13.28	-0.41	29.74	28.66	1.08
8	13.32	12.84	0.48	32.36	34.10	-1.74
9	11.31	11.37	-0.065	46.57	44.99	1.58

Table 5b. Theoretical (predicted) values and the observed (actual) values observed for responses, Y3 (bulk density) and Y4 (microparticle yield).

	Y3 (Bulk density (g/cc))			Y4 (Yield (%))		
	Actual value	Predicted value	Residual	Actual value	Predicted value	Residual
1	0.16	0.16	7.8×10^{-4}	67.62	70.18	-2.56
2	0.18	0.18	3.7×10^{-3}	69.21	63.89	5.32
3	0.20	0.21	-8.0×10^{-3}	40.73	51.29	-10.56
4	0.16	0.15	7.8×10^{-3}	65.02	57.92	7.10
5	0.17	0.17	-3.8×10^{-3}	57.80	51.62	6.18
6	0.20	0.20	1.2×10^{-3}	37.45	39.03	-1.58
7	0.11	0.14	-0.023	16.64	33.40	-16.76
8	0.17	0.15	0.021	33.94	27.10	6.84
9	0.18	0.18	-3.2×10^{-4}	20.53	14.51	6.02

distribution of DFS in EC matrix, synonymous to the matrix system.

Investigation of the droplet formation from the 3-F nozzle demonstrated that an inner rhodamine droplet was formed within a clear polymer coat. On drying, these droplets result in the formation of layered MP consistent with the internal morphology of microcapsules.

Examination of the effect of increasing TSC of the feed solution and FFR on the MP characteristics using the 3-F spray drying nozzle showed an increase in MP size and bulk density with an increase in TSC (**Table 4**, **Figure 5A – C**). Similarly, an increase in MP size with increasing TSC was observed when using a standard 2-F nozzle. This is as expected as an increase in feed solid concentration will give rise to an increase in feed viscosity resulting in larger and denser droplets and MPs [10,15,35]. A decrease in MP yield with an increase in TSC was consistent with the literature [35,36]. Tewa-Tagne *et al.* prepared microparticles containing polymeric nanocapsules and reported that an increase in Kollidon 30 from 5% to 10% w/v in the feed preparation caused a decrease in the yield from 63% to 59% [36].

Similarly, an increase in FFR led to a significant increase in MP size ($D_{90\%}$), and a decrease in yield (**Table 4**, **Figure 5B, D**). Likewise, when using a 2-F nozzle and a TSC of 10%, larger MP size and lowest MP yield was observed at the highest FFR rate of 10 mL/min. This was consistent with the literature. An increase in FFR was reported to result in an increase in size of DFS/ethylcellulose MPs, and of DFS/Eudragit RS30D MPs [4]. Similar observations were reported for Eudragit® MPs by Esposito *et al.* who also reported a corresponding decrease in the product yield. Both authors used a conventional 2-F nozzle spray drying [13].

Multiple linear regression analysis indicated a linear relationship for the effect of TSC and FFR on all responses except for $D_{50\%}$ where a quadratic model was valid. Analysis of residuals showed good validation of the model.

A higher EE at > 100% was observed for MPs formulated at high TSC for the 3-F nozzle, compared to the standard 2-F nozzle. This was related to the differences in viscosity of DFS and EC feed solutions resulting in an overall slightly lower FFR of the EC feed solution and hence higher DFS: EC ratio than 1:1.

For MPs from 3-F spray drying, DSC showed separate thermal events for the crystalline DFS and EC molecular mobility, demonstrating a heterogeneous structure, reflecting DFS in core and EC as coat and this is supported by TEM and FT-IR. DSC of MPs from 2-F spray drying showed that the DFS was molecularly dispersed throughout the EC

matrix and was supported by the recrystallisation of DFS at ~ 225°C. In addition, TEM showed that these MPs had homogeneous matrix structure, while FT-IR showed similarity of 2-F MPs to the corresponding PM.

These results therefore indicate that the novel 3-F nozzle results in the formation of microcapsules where the DFS is in the core surrounded by a coat of EC.

5. Conclusion

Spray drying using a novel 3-F nozzle was shown to result in MPs with differentiated internal morphology. The MPs from 3-F nozzle showed an inner core of crystalline drug coated by EC polymer, while MPs from conventional spray drying showed DFS as molecularly dispersed in EC matrix. Hence, it can be concluded that the novel 3-F nozzle results in the formation of multilayered and multifunctional MPs. The potential for forming microcapsules or coated MPs is attractive for multiple applications as it offers efficient environmental protection of the encapsulated core for enhanced stability/taste masking of bitter cores/actives and greater control of drug release because the drug is not located at the surface. This technology also allows formation of MPs with functionalised coating to enhance drug delivery and targeting. In addition, the 3-F nozzle can be used to formulate hollow/low density microcapsules for diagnostic and inhalation applications.

Declaration of interest

Z Ramtoola receives funding from Enterprise Ireland. The authors declare no conflict of interest.

Bibliography

1. Zhang Y-Z, Liao X-M, Yin G-F, et al. Preparation of water soluble drugs-loaded microparticles using modified solution enhanced dispersion by supercritical CO2. Powder Technol 2012;221:343-50
2. Heng D, Lee SH, Ng WK, Tan RB. The nano spray dryer B-90. Expert Opin Drug Deliv 2011;8(7):965-72
3. Mu L, Teo MM, Ning HZ, et al. Novel powder formulations for controlled delivery of poorly soluble anticancer drug: application and investigation of TPGS and PEG in spray-dried particulate system. J Control Release 2005;103(3):565-75
4. Rattes ALR, Oliveira WP. Spray drying conditions and encapsulating composition effects on formation and properties of sodium diclofenac microparticles. Powder Technol 2007;171(1):7-14
5. Peltonen L, Valo H, Kolakovic R, et al. Electrospraying, spray drying and related techniques for production and formulation of drug nanoparticles. Expert Opin Drug Deliv 2010;7(6):705-19
6. Masters K. Spray drying handbook. 3rd edition. Godwin G, London, UK; 1979
7. Bittner B, Kissel T. Ultrasonic atomization for spray drying: a versatile technique for the preparation of protein loaded biodegradable microspheres. J Microencapsul 1999;16(3):325-41
8. Cal K, Sollohub K. Spray drying technique. I: hardware and process parameters. J Pharm Sci 2010;99(2):575-86
9. Chen R, Okamoto H, Danjo K. Particle design using a 4-fluid-nozzle spray-drying technique for sustained release of acetaminophen. Chem Pharm Bull 2006;54(7):948-53
10. Raffin RP, Jornada DS, Ré MI, et al. Sodium pantoprazole-loaded enteric microparticles prepared by spray drying: effect of the scale of production and process validation. Int J Pharm 2006;324(1):10-18
11. Shigeyuki T, Yoshiaki U, Hajime T, et al. Preparation and characterization of copoly (dl-lactic/glycolic acid) microparticles for sustained release of thyrotropin releasing hormone by double nozzle spray drying method. J Control Release 1994;32(1):79-85
12. Finney J, Buffo R, Reineccius G. Effects of type of atomization and processing temperatures on the physical properties and stability of spray-dried flavors. J Food Sci 2002;67(3):1108-14
13. Esposito E, Roncarati R, Cortesi R, et al. Production of Eudragit microparticles by spray-drying technique: influence of experimental parameters on morphological and dimensional characteristics. Pharm Dev Technol 2000;5(2):267-78
14. He P, Davis SS, Illum L. Chitosan microspheres prepared by spray drying. Int J Pharm 1999;187(1):53-65
15. Clarke N, O'connor K, Ramtoola Z. Influence of formulation variables on the morphology of biodegradable microparticles prepared by spray drying. Drug Dev Ind Pharm 1998;24(2):169-74
16. Freiberg S, Zhu X. Polymer microspheres for controlled drug release. Int J Pharm 2004;282(1):1-18
17. Nagamine S, Sugioka A, Iwamoto H, Konishi Y. Formation of TiO_2 hollow microparticles by spraying water droplets into an organic solution of titanium tetraisopropoxide (TTIP) — Effects of TTIP concentration and TTIP-protecting additives. Powder Technol 2008;186(2):168-75
18. Jaworek A. Electrostatic micro-and nanoencapsulation and electroemulsification: a brief review. J Microencapsul 2008;25(7):443-68
19. Legako J, Dunford NT. Effect of spray nozzle design on fish oil–whey protein microcapsule properties. J Food Sci 2010;75(6):E394-400
20. Ramtoola Z. Method of producing microcapsules. WO2008056344; 2008
21. Ramtoola Z, Lyons P, Keohane K, et al. Investigation of the interaction of biodegradable micro-and nanoparticulate drug delivery systems with platelets. J Pharm Pharmacol 2011;63(1):26-32
22. Pabari RM, Ramtoola Z. Application of face centered central composite design to optimise compression force and tablet diameter for the formulation of mechanically strong and fast disintegrating orodispersible tablets. Int J Pharm 2012;430(1-2):18-25
23. Saravanan M, Bhaskar K, Maharajan G, et al. Development of gelatin microspheres loaded with diclofenac sodium for intra-articular administration. J Drug Target 2011;19(2):96-103

24. Shivakumar H, Desai B, Deshmukh G. Design and optimization of diclofenac sodium controlled release solid dispersions by response surface methodology. Indian J Pharm Sci 2008;70(1):22

25. Jelvehgari M, Barar J, Valizadeh H, Loveymi BD, Ziapour M. Preparation of diclofenac sodium composite microparticles with improved initial release property. Scientia Iranica 2010;17(2):79-89

26. Ravindra R, Krovvidi KR, Khan AA, Rao AK. FTIR, diffusivity, selectivity, and aging studies of interactions of hydrazine, water, and hydrazine hydrate with the ethylcellulose membrane. Macromolecules 1997;30(11):3288-92

27. Desai J, Alexander K, Riga A. Characterization of polymeric dispersions of dimenhydrinate in ethyl cellulose for controlled release. Int J Pharm 2006;308(1):115-23

28. Suthar V, Pratap A, Raval H. Studies on poly (hydroxy alkanoates)/(ethylcellulose) blends. Bull Mater Sci 2000;23(3):215-19

29. Pasquali I, Bettini R, Giordano F. Thermal behaviour of diclofenac, diclofenac sodium and sodium bicarbonate compositions. J Therm Anal Calorim 2007;90(3):903-7

30. Sipos P, Szucs M, Szabó A, Eros I, Szabó-Révész P. An assessment of the interactions between diclofenac sodium and ammonio methacrylate copolymer using thermal analysis and Raman spectroscopy. J Pharm Biomed Anal 2008;46(2):288-94

31. Hyppölä R, Husson I, Sundholm F. Evaluation of physical properties of plasticized ethyl cellulose films cast from ethanol solution Part I. Int J Pharm 1996;133(1):161-70

32. Lai HL, Pitt K, Craig DQM. Characterisation of the thermal properties of ethylcellulose using differential scanning and quasi-isothermal calorimetric approaches. Int J Pharm 2010;386(1-2):178-84

33. Rekhi SG, Jambhekar SS. Ethylcellulose-A polymer review. Drug Dev Ind Pharm 1995;21(1):61-77

34. Cwiertnia B, Hladon T, Stobiecki M. Stability of diclofenac sodium in the inclusion complex with β-cyclodextrin in the solid state. J Pharm Pharmacol 1999;51(11):1213-18

35. Goula AM, Adamopoulos KG. Spray drying of tomato pulp: effect of feed concentration. Drying Technology 2004;22(10):2309-30

36. Tewa-Tagne P, Briançon S, Fessi H. Preparation of redispersible dry nanocapsules by means of spray-drying: development and characterisation. Eur J Pharm Sci 2007;30(2):124-35

Affiliation

Ritesh M Pabari PhD, Tara Sunderland MSc & Zebunnissa Ramtoola† PhD
†Author for correspondence
School of Pharmacy,
Royal College of Surgeons in Ireland,
123, St Stephens Green,
Dublin 2, Ireland
Tel: +35314028626;
Fax: +3534022765;
E-mail: zramtoola@rcsi.ie